Bubble growth during subcooled nucleate boiling on a vertical heater: A mechanistic attempt to evaluate the role of surface characteristics on microlayer evaporation

Sarker, D.; Ding, W.; Hampel, U.;

Originally published:

May 2019

Applied Thermal Engineering 153(2019), 565-574

DOI: https://doi.org/10.1016/j.applthermaleng.2019.03.040

Perma-Link to Publication Repository of HZDR:

https://www.hzdr.de/publications/Publ-28110

Bubble growth during subcooled nucleate boiling on a vertical heater: A mechanistic attempt to evaluate the role of surface characteristics on microlayer evaporation

D. Sarker[a], W. Ding[a b], U. Hampel[a,b]
[a] Helmholtz-Zentrum Dresden-Rossendorf (HZDR), Institute of Fluid Dynamics, Bautzner Landstraße 400, 01328 Dresden, Germany
[b] Technische Universität Dresden, AREVA Endowed Chair of Imaging Techniques in Energy and Process Engineering, 01062 Dresden, Germany

Abstract:

For the modelling of nucleate boiling heat transfer, the bubble growth dynamics is of key importance. The study reported in this paper focuses on a qualitative assessment of the role of heater surface parameters on the bubble growth and the effective microlayer thickness constant, C_{eff}. The latter is part of a recently derived improved bubble growth model, which we utilize in our analysis along with high-resolution experimental data of the steam bubble growth. The bubble growth model is formulated considering the evaporation of microlayer beneath the bubble, heat diffusion at the bubble surface and condensation at the bubble cap. We found that the values of C_{eff} are lower and the growth rates of bubble prior to departure are greater at the root mean square roughness of around Sq=0.12 μm for low-wetting surfaces. For well-wetting surfaces C_{eff} and the bubble growth rates are also found lower and greater, respectively at Sq=0.15 μm. Finally, a generalized equation for C_{eff} is proposed which comprises the effects of surface roughness and wettability on the bubble growth. The findings are useful for improving the bubble growth models and in designing the heater surface in future.

Keywords: bubble growth model; surface wettability; optimal roughness; microlayer evaporation.

Nomenclature

A	model parameter	θ	subcooling factor, contact angle
b, $\acute{b}$	constant, model parameter	δ	thickness of thermal boundary layer (m)
c_p, C_2	specific heat capacity (J/ kg. K), constant	ν	kinematic viscosity (m²/s)
d, D	diameter (m)	ρ	density (kg/m^3)
g	gravitational acceleration (=9.81 m/s^2)	ϕ	function of fluid parameters and microlayer constant (K)
h	heat transfer coefficient (W/m².K)	ψ	function of fluid properties (K)
h_{lv}	latent heat of evaporation (J/kg)	ζ	coefficient for flow boiling phenomena
Ja	Jakob number (dimensionless)		
k	thermal conductivity (W/m.K)	*Subscripts*	
L	thickness of hydrodynamic boundary layer (m)	*adv*	advancing
m	constant	*b*	bubble, bubble surface
Pr	Prandtl number (dimensionless)	*c*	condensation, conduction
q''	heat flux (W/m²)	*d*	departure
R, R^+	radius (mm), nondimensional bubble radius	*eff*	effective
Re	Reynolds number (dimensionless)	*i*	interface
$\acute{S}$	portion of bubble in contact with subcooled liquid (dimensionless)	*l*	bulk liquid

Sq	root mean square roughness of surface (μm)	*ml*	microlayer
t, t^+	time (sec), nondimensional time	*rec*	receding
T	temperature (K)	*sat*	saturation
		v	vapor
		w	heater surface, waiting period
Greek Symbols		*x*	normal to the heater wall
α	thermal diffusivity (m²/s)	*0*	initial
ΔT	liquid superheat (K)	∞	superheated liquid layer

1. Introduction

Bubble dynamics and the associated heat transfers in heterogeneous nucleate boiling have been widely investigated over the past six decades. The general consensus among researchers is that a simple nucleated bubble life cycle includes nucleation, growth, departure, sliding and detachment from the heater surface. Below we will briefly summarize the basic physics of the bubble growth process based on the existing literature and the scope of the present study.

In 1917, Lord Rayleigh [1] solved one dimensional momentum interaction between the bubble and the surrounding fluid. Liquid inertia was utilized as the limiting force for the bubble growth in his model. Lien and Griffith [2] later divided the total bubble growth period in two stages; initial and final growth period. In the initial stage, the hydrodynamic effects dominate the growth process due to the surface tension forces around the bubble surface. The bubble shape could be hemispherical [3] and a so-called microlayer forms beneath the nucleated bubble in this period. While height of a nucleated bubble is smaller than the thickness of a superheated liquid layer on the heater surface (δ_w), significant mass transfer takes place from this layer to the bubbles. Consequently, a bubble grows rapidly within the first few milliseconds [4] and pushes the surrounding liquid outward. As an effect, a thin unsteady thermal boundary layer develops between the saturated bubble dome and the surrounding liquid [5]. Zuber [6] postulated that the thermal boundary layer (δ_l) develops as the thermal waves advances from the vapour bubble interface to the liquid and reaches the outer limit of the hydrodynamic boundary layer (*L*). The bubble-liquid interfacial temperature drops from the superheat to the saturation temperature due to the rapid expansion of the bubble surface. Mayinger [4] observed such temperature gradient around the bubble after 1.3 ms of a bubble generation. Fig. 1 illustrates the superheated liquid layer around a growing bubble in an infinite bulk liquid and on a vertical heater.

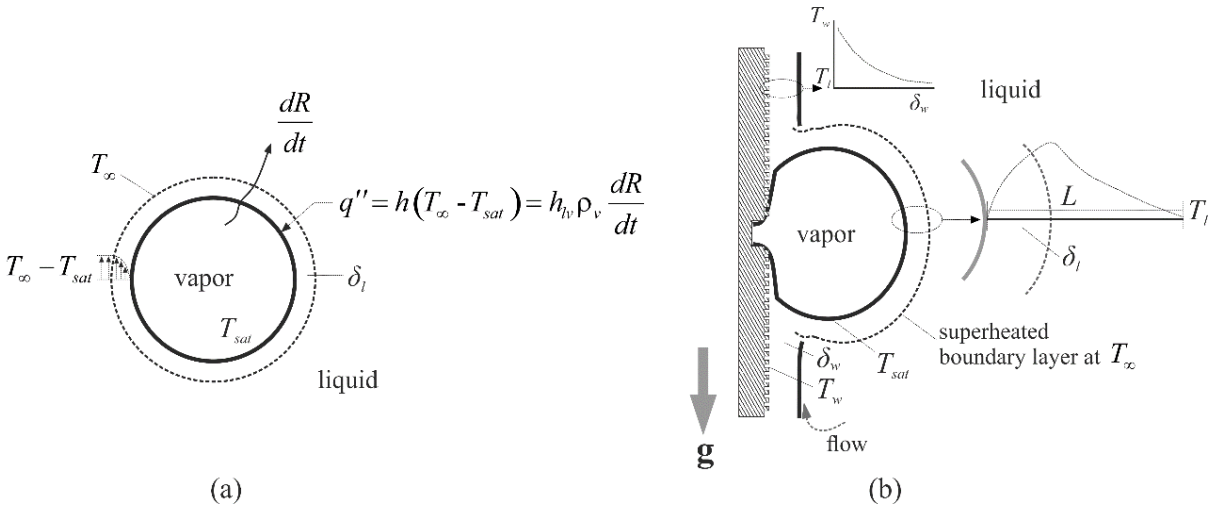

Fig. 1: Bubble growth mechanisms based on the classical models [6-9], left (a): in an infinite bulk of uniformly superheated liquid and right (b): on a vertically oriented heater in a non-uniform temperature field.

During the final growth period, the superheated thermal boundary layer surrounding a bubble (δ_l) supplies substantial heat to the bubble through the bubble-liquid interface and facilitates the bubble growth, is known as heat diffusion (q_l''). In a non-uniform temperature field, a part of heat transfers from the vapor interface to the bulk liquid (q_b''). The microlayer underneath the bubble base evaporates (q_{ml}'') in this stage as well and contributes in the growth of a bubble. Hence, at the beginning of the final growth period, a large amount of heat transfers to the bubble. Fig. 2 briefly demonstrates the heat transfer mechanisms, which control the bubble growth. The interfacial velocity of bubble surface is slowed down and the thermal energy of the boundary layer around the bubble surface decreases in the final stage of the bubble growth period [3]. Koffman and Plesset [10] and Jung and Kim [11] conducted experiment using degassed deionized water in subcooling conditions at atmospheric pressure and stated that the microlayer contributes around 50% and 17% of the total energy from the wall to the bubble, respectively. The general consensus is that the contribution of the superheated liquid surrounding the bubble (q_l'') is greater than the microlayer evaporation (q_{ml}'') in bubble growth and departure during subcooled nucleate boiling [11, 12]. However when the bubble diameter increases considerably, the top of the bubble passes through the saturated layer of liquid and enters into the subcooled bulk liquid region. Then, condensation heat transfer (q_c'') takes place at the bubble cap in this situation (Fig. 2). A further consideration could be that the condensation at the bubble cap may not start as soon as the bubble height is greater than the thickness of the superheated liquid layer. The reason is that a growing bubble pushes the superheated liquid layer outward and the bubble still stays within the envelope of this layer. Temperature gradients inside and outside of this superheated liquid layer were observed by some investigators [13, 14]. Since a growing bubble stretches the superheated liquid layer and its total distance depends on the bubble height, we have represented it as a function of a bubble height ($m.D_x$) in our study. Here D_x is the height of a bubble and m is the fraction of the bubble height that is covered by the superheated thermal boundary layer. As long as, the total mass due to the microlayer evaporation and the heat diffusion through bubble surface exceeds the condensation mass, the bubble continues to grow. The condensation effect becomes significant and the bubble growth rate will be gradually reduced, as a large portion of the bubble top is exposed to the subcooled bulk liquid. Main parameters which determine the contribution of microlayer evaporation on the bubble growth are the fluid properties (such as latent heat of vaporization) [12], liquid subcooling, system pressure [15], and surface characteristics [16]. Few recent works investigated the effects of heater surface characteristics on the microlayer evaporation [17, 18]. Several other attempts were made to find-out the impact of heater surface characteristics on the bubble growth dynamics [19-22]. The interactions between the surface profile and the microlayer beneath a nucleated bubble play a prominent role in the heat transfer when the height of the surface roughness and microlayer thickness are of similar (micrometer) length scale. According to our best knowledge, the influences of solid material properties were not widely incorporated in the bubble growth models. In this article, the role of heater surface roughness (root mean square roughness of the surfaces in the range of 0.004 μm to 0.46 μm) for low-and well-wetting surfaces on the bubble growth during nucleate boiling were studied. For that we compared experimentally measured bubble sizes of our previous studies [23, 24] against the numerically calculated bubble sizes and inferred heater surface effects on the bubble growth during nucleate boiling. A key parameter in this analysis is the so-called effective microlayer thickness constant, C_{eff}, for which we derive an expression that includes surface wettability and root mean square roughness of the surface (Sq). In the following section, we will start with a brief review of the existing bubble growth models.

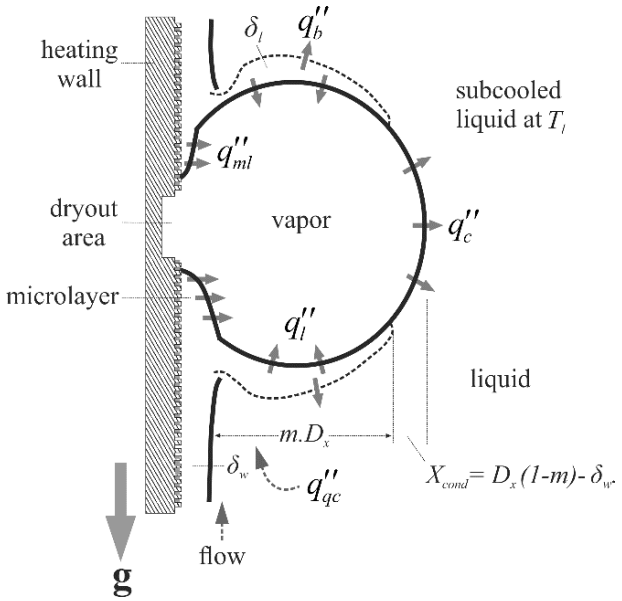

Fig. 2: Relevant heat transfers during the growth of a bubble on a cavity.

2. Bubble growth models

Bubble growth models were developed on the basis of different mechanisms, such as, liquid inertia, heat diffusion, microlayer evaporation and condensation. Liquid inertia was postulated as the controlling factor for the bubble growth in few former models. Some models suggested that the bubble behavior is governed by the heat diffusion from the superheated liquid layer around a bubble in its growth [7-9]. A number of heat diffusion based bubble growth models were developed for a bubble growing in an infinite bulk of superheated liquid [7, 9], whereas Zuber [6] suggested that the hydrodynamic and the energy aspects should be taken into account together while a bubble grows on a heating surface. Additionally, the effects of surface tension, viscosity and contact angle should be included in the bubble growth models. Mei et al. [25] asserted that most of the energy transferred to the bubble goes through the microlayer. Hence this effect has to be included into the bubble growth models. Their further finding was that the energy transfer to the bubble decreases over time due to the larger heat release rate by a departing bubble than the supplied energy from the heater. Therefore, the actual bubble growth rate becomes slower than the predicted one. Few other groups combined the effects of microlayer evaporation and heat diffusion at the bubble surface to derive the expressions for the bubble growth [26]. The temperature field in the liquid near the bubble boundary during subcooled boiling was observed to be changed noticeably [27, 28]. Chen and Mayinger [27] added that the condensation rate at the bubble surface varies with the latent heat of vaporization of different working fluids. Hence, different groups recommended adding a convective term in the bubble growth models and incorporated the condensation effects in their bubble growth models [5, 29, 30]. Table 1 summarizes the most prominent bubble growth models.

Table 1: Bubble growth models.

Author	Model	Features
Plesset and Zwick [7]	$\frac{dR(t)}{dt} = \sqrt{\frac{3}{\pi}} Ja \left(\frac{\alpha}{t}\right)^{0.5}$. $Ja = \frac{T_w - T_{sat}}{h_{lv}\rho_v} c_{pl}\rho_l$. $\alpha = \frac{k_l}{\rho_l c_{p,l}}$.	• bubble is assumed spherical throughout its growth and has uniform temperature and pressure. • compressibility and viscous effects are neglected in the bubble growth mechanisms.
Zuber [6]	$\frac{dR(t)}{dt} = \frac{b}{\sqrt{\pi}} Ja \left(\frac{\alpha}{t}\right)^{0.5}$. '$b$'is the correction factor for sphericity.	• $1 \le b \le \sqrt{3}$ is valid for the saturated bulk liquid at atmospheric pressure and at low wall heat flux.
	$\frac{dR(t)}{dt} = \frac{b}{\sqrt{\pi}} Ja \left(\frac{\alpha}{t}\right)^{0.5} - b\frac{q''_b}{h_{lv}\rho_v}$.	• bubbles grow on a heated surface in non-uniform temperature field. • heat transfers in two opposite directions; from

	'q_b''' is the heat flux from the vapor interface to the bulk liquid.	the surrounding superheated liquid layer (T_∞) to the saturated bubble interface (T_{sat}) and from the bubble interface (T_{sat}) to the bulk liquid (T_l).
Mikic et al. [31]	$dR(t)=A.dt$; $t^+ \ll 1$ $dR(t)=B.\sqrt{dt}$; $t^+ \gg 1$ $t^+ = \frac{A^2 t}{B^2}$. $A=\left(\acute{b}\frac{h_{lv}\rho_v \Delta T}{\rho_l T_{sat}}\right)^{\frac{1}{2}}$, $B=\left(\frac{12}{\pi}\alpha_l\right)^{\frac{1}{2}} Ja$.	• the total kinetic energy of the moving liquid by a bubble is equivalent to the work done at the bubble-liquid boundary. • bubbles start to grow from zero radius rather than a critical radius on a surface. • both the liquid inertia and heat transfer controlled growth stages are included.
	$\frac{dR(t)}{dt}=\frac{1}{2}\frac{B}{\sqrt{t}}\left[\frac{T_w-T_{sat}}{\Delta T}-\theta\left(\frac{t}{t+t_w}\right)^{1/2}\right]$. $\theta=\frac{T_w-T_l}{T_w-T_{sat}}$.	• bulk liquid of uniform temperature (T_l) comes in contact with the hot surface (T_w) and after certain period of time (t_w), a bubble forms and grows.
Cooper [15]	$\frac{dR(t)}{dt}=\frac{2}{C_2}\frac{T_{w,0}-T_{sat}}{\phi}\left(\frac{\nu_l}{t}\right)^{0.5}$. $\phi=\psi\left\{1+\frac{2}{C_2^2}\frac{c_{pl}(T_{w0}-T_{sat})}{h_{lv}}.\frac{1}{Pr_l}\right\}$. $\psi=\frac{\rho_v}{\rho_l}\frac{h_{lv}}{c_{pl}}Pr_l$. C_2=0.8.	• bubbles solely grow due to the evaporation of microlayer that exists beneath the bubble base. • dryout area in the microlayer is included. • thermal capacity of the microlayer is neglected.
Yun et al. [29]	$\frac{dR(t)}{dt}=\frac{2b}{\sqrt{\pi}}Ja\left(\frac{\alpha}{t}\right)^{0.5}-\frac{b\acute{S}\,q_i''}{h_{lv}\rho_v}$. $q_i''=h_c\left(T_{sat}-T_i\right)$, $h_c=\frac{k_l}{d_b}\left(2+0.6Re^{0.5}Pr^{0.3}\right)$. b=1.56, $\acute{S}$=0.5.	• heat diffusion at the bubble surface and the condensation at bubble cap work together during the bubble growth. • half of the bubble surface is assumed to be in contact to the subcooled bulk liquid. • microlayer evaporation and dryout in microlayer are not taken into account.
Colombo and Fairweather [30]	$\frac{dR(t)}{dt}=\frac{1}{C_2}JaPr_l^{-0.5}\left(\frac{\alpha}{t}\right)^{0.5}$ $+\sqrt{\frac{3}{\pi}}k_l\left(T_\infty-T_{sat}\right)\left(\frac{\alpha}{t}\right)^{0.5}\left(1-\acute{S}\right)-\frac{\acute{s}\,q_i''}{h_{lv}\rho_v}$. C_2=1.78.	• microlayer evaporation, heat diffusion and condensation heat transfer contribute in the bubble growth. • dryout area in the microlayer is not considered.
Raj et al. [32]	$\frac{dR(t)}{dt}=\frac{1}{C_2}\left(JaPr_l^{-0.5}\right)\left(\frac{\alpha}{t}\right)^{0.5}$ $+\sqrt{\frac{3}{\pi}\frac{k_l(T_\infty-T_{sat})}{\rho_v h_{lv}\alpha^{0.5}}}\left(\frac{1}{t}\right)^{0.5}\left(1-\acute{S}\right)-\frac{\acute{S}\,q_i''}{h_{lv}\rho_v}$.	• microlayer evaporation, heat diffusion and condensation heat transfer play role in the growth of a bubble. • dryout area is not taken into account.
Mazzocco et al. [33]	$\frac{dR(t)}{dt}=\left[\frac{\pi^2+1}{\pi^2\sqrt{\pi}}\frac{1}{\sqrt{Pr_l}}Ja\sqrt{\alpha}+\zeta\sqrt{\frac{3}{\pi}}Ja_w\sqrt{\alpha}\right]\left(\frac{1}{t}\right)^{0.5}$. $\zeta=-0.05\frac{T_{sat}-T_{bulk}}{T_{wall}-T_{sat}}$.	• heat addition due to the microlayer evaporation and heat transfer with the surrounding liquid are included in the modelling of bubble growth. • the condensation effects are considered based on existing data bases. • dryout area is not incorporated in the model.

None of the models in Table 1 includes the effects of heater surface characteristics, though the surface wettability and roughness have great impacts on the bubble growth dynamics [21-23, 34-36]. Generally, bubbles grow faster on the hydrophobic surfaces than that on the hydrophilic ones. The reason is that the surface tension at the three-phase line acts outwards for the hydrophobic surfaces [36]. Therefore, the bubble base areas are larger for the hydrophobic surfaces than that of the hydrophilic surfaces. The extended area of surface is susceptible to the heat transfer and increases the bubble growth rate. It may also influence the liquid flow in the microlayer and affects the bubble growth this way. In one of our recent reports [23], we showed that surface roughness influences the bubble growth via bubble base diameters and the bubble growth rate is the maximum for the optimal roughness. The optimal roughness ($Sq \approx 0.10$ μm) is the height of roughness where heat

extraction rates by bubbles are the maximum. Cooper [15] deduced an expression for the initial microlayer thickness on a smooth surface that includes a constant C_2. The value of C_2 was found in the range of 0.33 to 0.50 and 0.50 to 1.0 for the experimental results of Koffman and Plesset [10] and Cooper and Llyod [37], respectively. The influence of microlayer on the bubble growth does not depend only on the initial microlayer thickness, but rather the effective interaction between the microlayer and the heater surface profile. Therefore, we propose a term C_{eff} instead of C_2 for capturing the effective contributions of heater surface characteristics on the bubble growth prior to departure. C_{eff} also denoted as the effective microlayer thickness constant in the present study. During the evaporation of microlayer, a dryout area appears in the microlayer [11, 15, 38]. Yabuki and Nakabeppu [12] claimed that high heat transfer occurs at the three-phase contact line of the dryout area for liquids with low latent heat. If the impact of the dryout area is not taken into account, the overvalued microlayer evaporation area leads to the overestimation of the microlayer contribution to the bubble growth. That is, the term C_{eff} will be overestimated. Cooper [15] derived expressions of the bubble sizes with the dryout area. In our study, we have used the expression of microlayer evaporation that includes the dryout area, whereas few recent studies [32, 33] did not take it into account. Cooper [15] and Cooper and Llyod [39] addressed the effects of inertia, viscosity, surface tension and neglected the thermal capacity of the microlayer during the analysis of the microlayer formation and evaporation. They quantified the contributions of these effects and found that their effects for the bubble growth are counter-acting in different orders. For the simplicity of the analysis, they concluded that the initial wall superheat is the most significant. CFD analysis of Hänsch and Walker [40] also showed that the microlayer thickness is positively correlated with the liquid viscosity and negatively correlated with the surface tension. Jung and Kim [41] recently proposed an advanced model of initial microlayer thickness, which incorporates the effects of surface tension force, bubble shape and residual flow. They found that the model of initial microlayer thickness by Cooper and Llyod [39] performs better against Jung and Kim [41]'s experimental results comparing to the other models [42, 43]. As the values of C_{eff} were derived for different heater surfaces in the present study instead of assuming any constant, the determined values incorporate the effects of heater surface characteristics. Hence we used the expression of accounting the contribution of microlayer evaporation in the bubble growth, suggested by Cooper [15] as a sub-model in the present bubble growth model. We have also adopted the correlation of Mikic et al. [31] as a sub-model to account the heat transfer to the bubble that transfers through the bubble-liquid interface. This model coupled both the inertia and heat diffusion controlled bubble growth with the help of Clausius-Clapeyron equation. It is a distinguishable feature compare to the bubble growth model of Plesset and Zwick [7]. For the sake of simplifications, heat transfer from the superheated thermal layer (δ_l) to the bulk liquid $\left(q_b''\right)$ is neglected in the model. Once q_b'' is neglected, then it can be considered that a bubble grows in a uniformly heated liquid. Zuber [6] found that the effects of liquid inertia and surface tension are not important, while a bubble grows in uniformly heated liquid.

The condensation heat transfer plays an important role in the bubble growth by releasing heat from the bubble to the subcooled liquid. The condensation effects are also yet to be taken into account properly in some models. During subcooled nucleate boiling, the effects of condensation should be included in the bubble growth model. The pioneering correlation of Ranz and Marshall [44] is widely used in CFD models. The same condensation correlation is also used in the other bubble growth models (Table 1), though the model was developed for spherical water droplets evaporating in air. It is

$$Nu_c = 2 + 0.6 Re_b^{0.5} Pr^{0.3}. \quad Re_b < 200 \qquad 1(a)$$

The models for the condensation of steam bubbles in liquid water were developed by different groups for a wide range of Reynolds number, Jakob number and bubble diameter. Since the liquid subcooling and the relative bubble velocities of our experimental cases were very low, we used Chen and Mayinger [27] and Ranz and Marshall [44]'s correlations for the present bubble growth model. The correlation of Chen and Mayinger [27] is

$$Nu_c = 0.185 Re_b^{0.7} Pr^{0.5}. \quad 100 < Re_b < 10000 \qquad 1(b)$$

Considering all the above mentioned facts and the relation of the thickness of superheated liquid layer around the bubble surface ($m.D_x$), we have formulated the expressions for the bubble growth. For this, three different models [15, 31, 44] are used as sub-models in our bubble growth model which represent the associated mechanisms of the bubble growth. The proposed bubble growth model is as follows

when $D(t) < \delta_w + m.D_x$,

$$\frac{dR(t)}{dt} = \frac{2}{C_{eff}} \frac{T_{w0}-T_{sat}}{\phi} \left(\frac{\nu_l}{t}\right)^{0.5} + A.\ t^+ \ll 1 \quad 2(a)$$

$$\frac{dR(t)}{dt} = \frac{2}{C_{eff}} \frac{T_{w0}-T_{sat}}{\phi} \left(\frac{\nu_l}{t}\right)^{0.5} + \frac{B}{\sqrt{dt}}.\ t^+ \gg 1 \quad 2(b)$$

when $D(t) > \delta_w + m.D_x$,

$$\frac{dR(t)}{dt} = \frac{2}{C_{eff}} \frac{T_{w0}-T_{sat}}{\phi} \left(\frac{\nu_l}{t}\right)^{0.5} + A\left(1-\acute{S}(t)\right) - \frac{\acute{S}q''_i}{h_{lv}\rho_v}.\ t^+ \ll 1 \quad 2(c)$$

$$\frac{dR(t)}{dt} = \frac{2}{C_{eff}} \frac{T_{w0}-T_{sat}}{\phi} \left(\frac{\nu_l}{t}\right)^{0.5} + \frac{B}{\sqrt{dt}}\ \left(1-\acute{S}(t)\right) - \frac{\acute{S}q''_i}{h_{lv}\rho_v}.\ t^+ \gg 1 \quad 2(d)$$

Here $A = \left(\acute{b}\frac{h_{lv}\rho_v \Delta T}{\rho_l T_{sat}}\right)^{\frac{1}{2}}$, $B = \left(\frac{12}{\pi}\alpha_l\right)^{\frac{1}{2}} Ja$. The portion of the bubble being in contact with the subcooled liquid is a function of δ_w and $m.D_x$. We have deduced it here as $\acute{S}(t) = 1 - \left(\frac{\delta_w}{D(t)} + m\right)$ where $\delta_w = 2\left(\frac{\alpha t_w}{\pi}\right)^{0.5}$ [45]. The proposed bubble growth models of the present study are shown in Eqns. 2. Eqns. 2 (a, b) are suitable for the bubbles which are within the superheated liquid layer and Eqns. 2 (c, d) are useful for the bubbles which are in contact with the subcooled bulk liquid. $t^+ \left(= \frac{A^2 t}{B}\right)$ defines the inertia force and heat diffusion controlled bubble growth regions. Eqns. 2 (c, d) show the sub-models of three heat transfer mechanisms which contribute in the bubble growth. The first, middle and last part of the Eqns. 2 (c, d) represent the microlayer evaporation with dryout area, heat diffusion through the bubble surface with liquid inertia and condensation at the bubble cap; respectively.

3. Calculation of C_{eff}

The three sub-models of the bubble growth model (Eqns. 2 c, d) consist of three constants (C_{eff}, $\acute{b}$ and $\acute{S}$). In the calculation of C_{eff}, $\acute{b}$ will be kept as constant for all the conditions. Mikic et al. [31] derived $\acute{b}$ as $\pi/7$ for a growing bubble attached to a heater surface by equating the work done on the surrounding liquid of a bubble and the kinetic energy of liquid mass. Hence in the calculation of this study $\acute{b}$ is considered as $\pi/7$. $\acute{S}$ is a constant of the equation for the contribution of condensing heat transfer which resembles the portion of a bubble in contact with the subcooled bulk liquid. Raj et al.[32] calculated that around 50% of a bubble enters into the subcooled liquid region at low heat flux, mass flux and subcooling. Yun et al. [29] also assumed the same value for their calculation. Therefore, we have calculated C_{eff} for the wide range of m=40%~55%, to check the significance of $\acute{S}$ on C_{eff}. Fig. 3 shows the calculation method of the bubble growth during nucleate boiling at low subcooling.

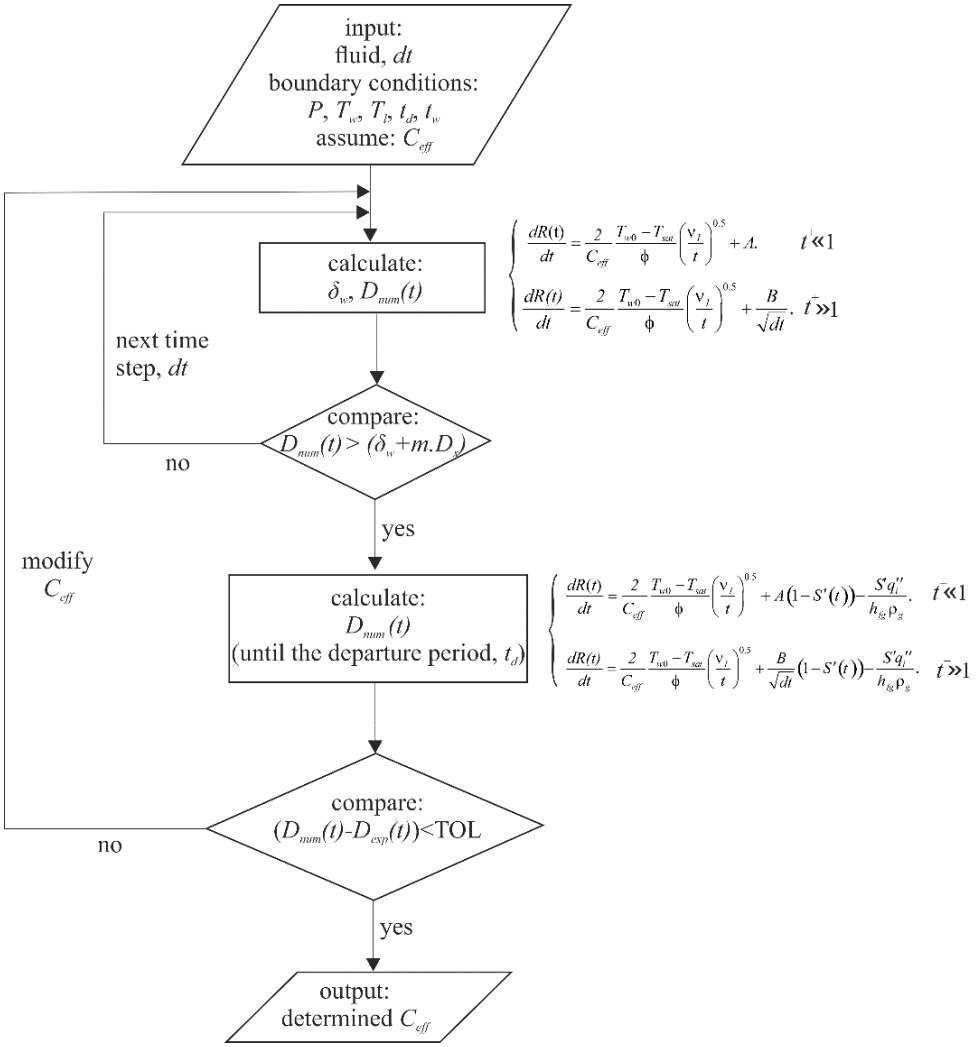

Fig. 3: A flowchart to determine the surface characteristics effects (C_{eff}) on the bubble growth.

The different boundary conditions of our former experimental studies [23, 24] on isolated nucleated bubbles, namely system pressure (P), bulk liquid temperature (T_l), heater wall temperature (T_w), bubble departure period (t_d), waiting period (t_w) and time step (dt) are employed in the model. The experiments were performed on the stainless steel surfaces of 0.5 mm thickness. The heater surfaces were treated with self-assembled monolayer (SAM) coating, wet-etching and femtosecond pulsed laser to alter the surface wettability and the roughness. Surface wettability and roughness were analyzed by a goniometer (Dataphysics OCA 30) and a confocal microscopy (μsurf explorer, xy-resolution: 0.3-3 μm, z-resolution: 3 nm); respectively. We measured the advancing (θ_{adv}) and receding (θ_{rec}) liquid contact angle and subtracted them to acquire the liquid contact angle hysteresis (θ_{hys}). Surface wettability was characterized by liquid contact angle hysteresis (θ_{hys}). Surface roughness was presented with the root mean square roughness of surface (Sq). The characteristics of heater surfaces are shown in Fig. 4. The total area of the heater surface was 130x20 mm². An artificial cavity was prepared on the patterned surface to generate bubble in a specific position. The boiling experiments were carried out in a borosilicate glass vessel at atmospheric pressure with deionized water. A schematic of the test section is shown in Fig. 5. Test heaters were fixed in vertical orientation. Before conducting the experiments, the test heaters and the glass vessel were cleaned properly. The deionized water in the glass vessel was degassed by an electric oven underneath the glass vessel. The subcooling (2-4 K) of the test liquid was controlled by the same electric oven. The bulk liquid temperatures were measured by K-type thermocouples. The test heaters were directly heated via. copper contacts and the heat flux from 19.22 kW/m² to 30.29 kW/m² were applied to nucleate the single bubbles from the artificial cavities. The liquid velocity fields generated by the heating were measured with particle image velocimetry (PIV) technique. The area- and time-averaged heater wall temperatures were determined by K-type thermocouple and infrared thermometry as well. The bubble life cycle was recorded by high resolution optical shadowgraphy. We used the image processing software ImageJ to

process the image stacks. The details of the surface preparation, analyzing and the boiling experiments can be found in [23, 24, 46, 47].

In the model (Fig. 3), Refprop 7.0 is used to calculate the fluid properties for different temperatures. Firstly, a value of C_{eff} is assumed. Then the bubble sizes are calculated for this assumed value of C_{eff} with different given m (40% ~55%) using Eqns. 2(a, b). The thickness of the superheated liquid layer on the heater surface (δ_w) is assessed and checked whether the bubble height is within the superheated liquid layer (δ_w). If the bubble is in the superheated layer, the calculation goes on for the next time step. When the calculated bubble height (D_x) is greater than the total thickness of superheated liquid layer ($\delta_w + m.D_x$), then the condensation heat transfer comes into play. However the bubble size is calculated for the each time step (dt=0.40 ms) and continues until the summation of time steps is equal to the total bubble departure period (t_d). The deviations between the experimental and the calculated bubble sizes for each time step are evaluated and averaged afterwards. The underestimated C_{eff} results larger bubble sizes. Therefore, the values of C_{eff} are iterated according to the discrepancies of calculated and experimental bubble sizes. When they agree well, the iterated C_{eff} value is considered as the desired one.

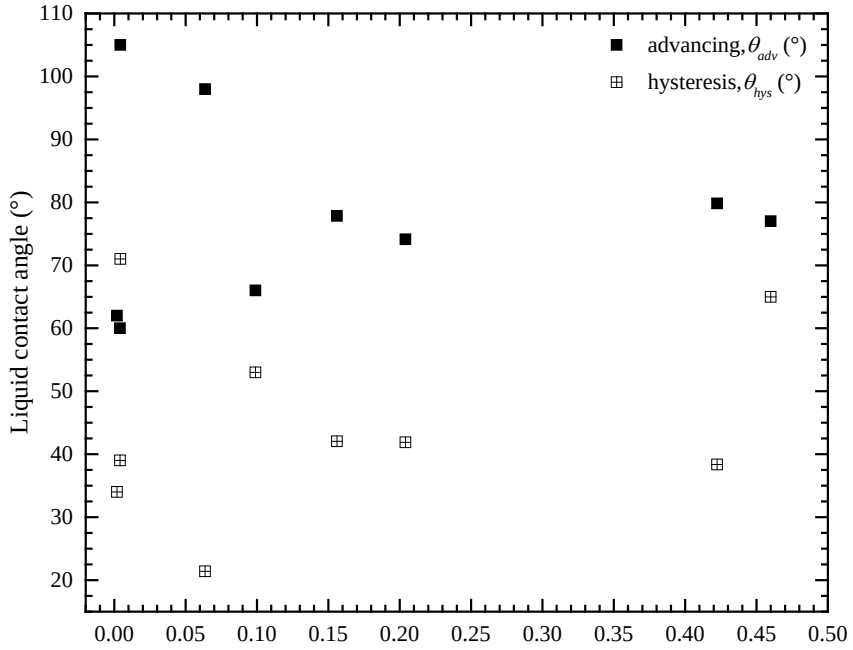

Fig. 4: Characteristics of heater surfaces.

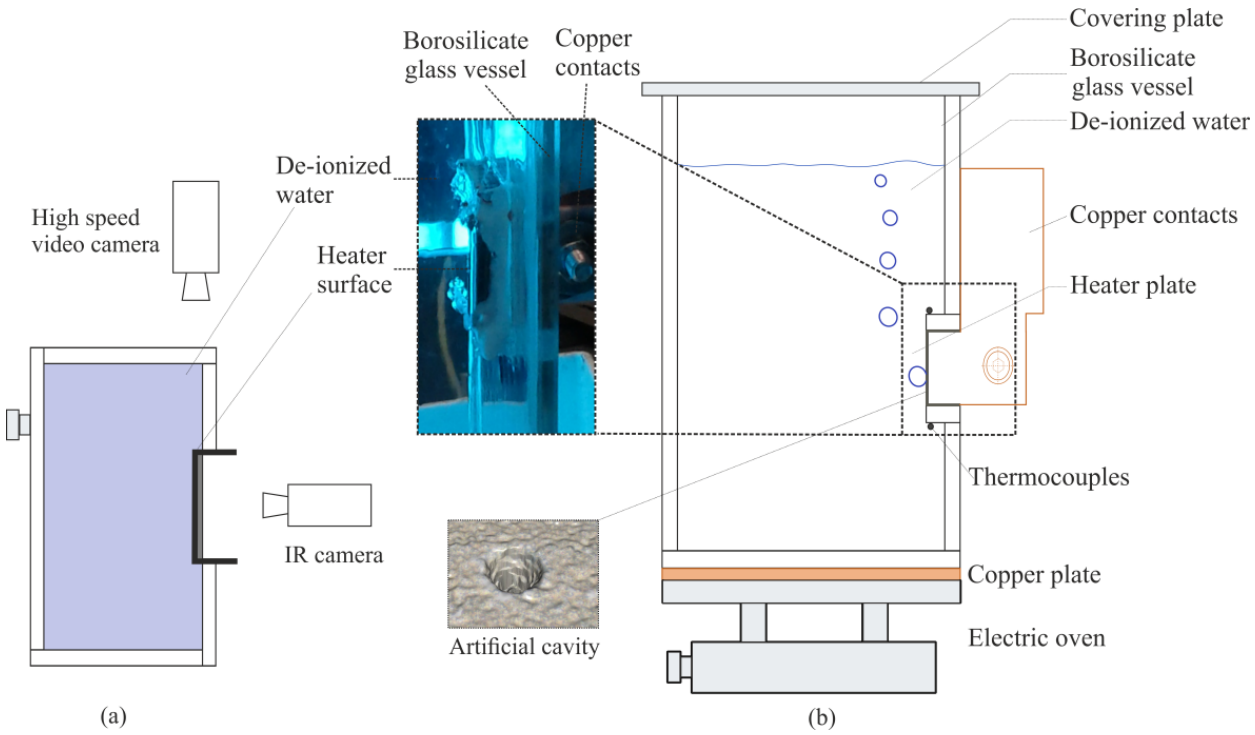

Fig. 5: Schematic of the test section top view (a) and side view (b) (adopted from Sarker et al. [24]).

4. Results and discussion

The numerically estimated bubble sizes are presented in this section. A generalized expression for an effective microlayer thickness constant (C_{eff}) is also developed here as a function of the liquid contact angle hysteresis (θ_{hys}) and the root mean square roughness of the surface (Sq). C_{eff} may get influenced by the portion of a bubble upon the condensation heat transfer ($\acute{S}$). Hence $\acute{S}$ is evaluated here first.

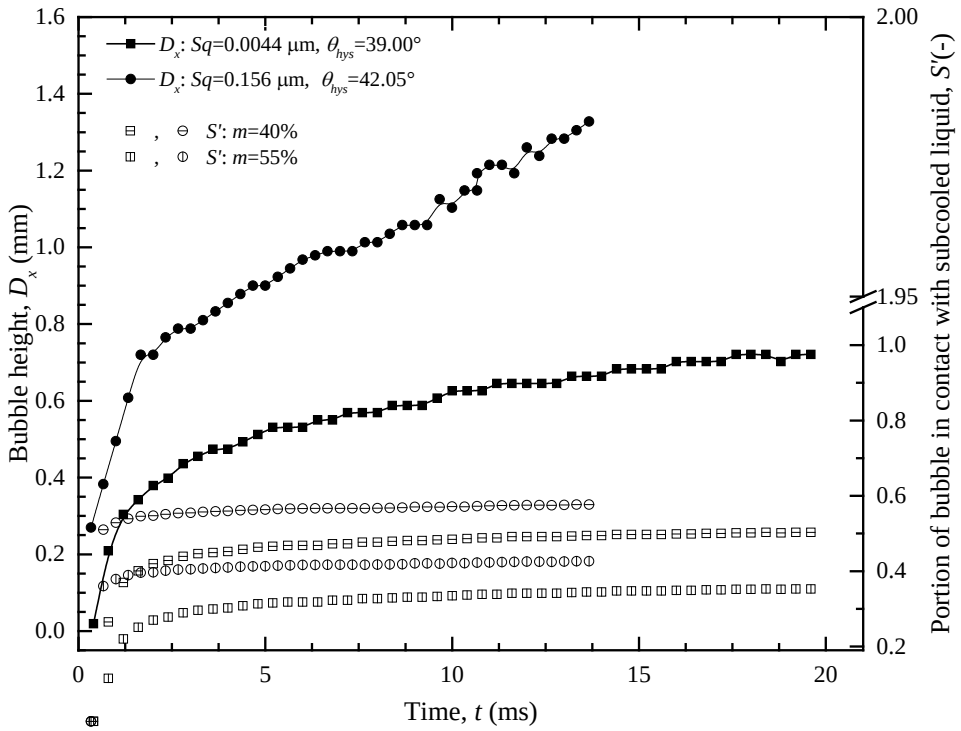

Fig. 6: Temporal evolution of bubble diameter and portion of condensing area (q'' =22.64 kW/m², ΔT_{sup}=7.50 K, ΔT_{sub}=3.00 K).

Fig. 6 shows the temporal evolution of $\acute{S}$ for the bubbles on two different heater surfaces and the corresponding bubble sizes. We see that $\acute{S}$ is in the range of 0.20 to 0.65 while the values of m are in the range of 40% to 55%. The portion of bubble in contact with the subcooled bulk liquid is greater while the bubble grows faster. The slope of the $\acute{S}$ curves increases at the beginning of the growth period. After 2.5 ms of the bubble growth period, the bubble growth rates are slowed down and the slope of $\acute{S}$ reduces. Additionally when the fraction of the superheated liquid layer around a bubble surface is assumed lower (m=40%), the condensation rate of a bubble increases. In the estimation of $\acute{S}$, there might be a limitation is that we have assumed a constant value of m for a growing bubble until its departure. But the temporal evolution of a bubble growth rate is not linear. As a result, some deviations may arise from this assumption. However, we have predicted the bubble sizes and the effects of heater surface characteristics on the bubble growth (C_{eff}) for a range of $\acute{S}$ values. The intention of considering a range of $\acute{S}$ values is to take the uncertainties into account which may originate from the calculation of $\acute{S}$.

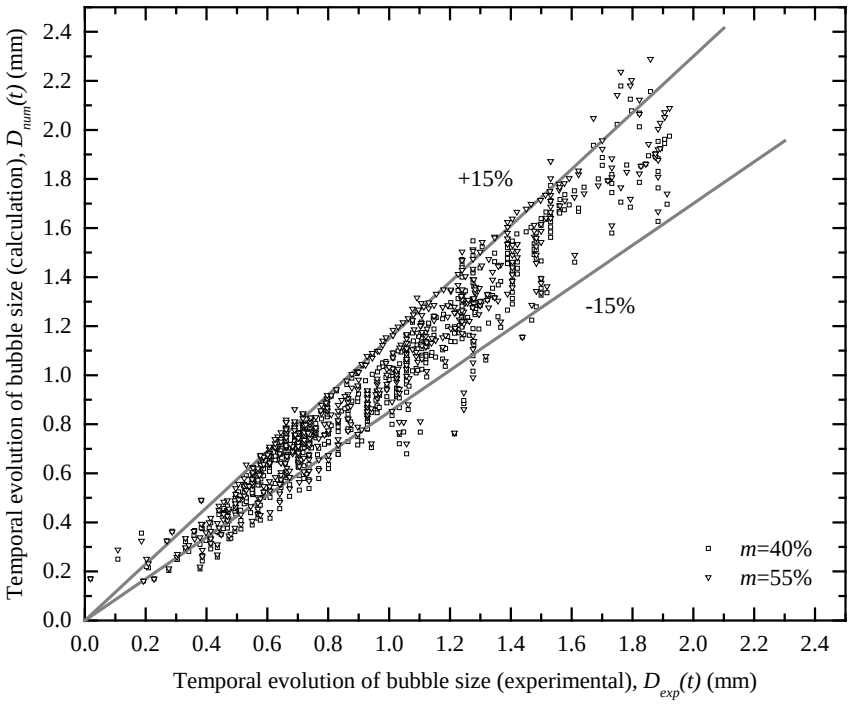

Fig. 7: Comparison of the experimentally and numerically estimated bubble sizes.

The comparison of our proposed bubble growth model (Eqns. 2 a,b,c,d) against the experimental results [23, 24] is shown in Fig. 7. We have found that 90.43% of numerically calculated bubble sizes lie within ±15% of error. Based on this agreement of the experimental and the numerical bubbles, the derived C_{eff} values are evaluated. Fig. 8 shows the values of C_{eff} for the surfaces of different wettability and roughness, while the m is in between 40% and 55%. We have not found a significant impact of m values or condensation at the bubble cap on the effective microlayer thickness constant (C_{eff}). The values of C_{eff} are found higher for the well-wetting surfaces than that of low-wetting surfaces. C_{eff} is minimum when the root mean square roughness of surfaces are approximately of Sq=0.12 μm and 0.15 μm for the low- and well-wetting surfaces, respectively. The values of C_{eff} increase for the smooth surfaces and for the surfaces with greater roughness than the above-mentioned limit (Sq=0.12 μm for the low-wetting surfaces and Sq=0.15 μm for the well-wetting surfaces).

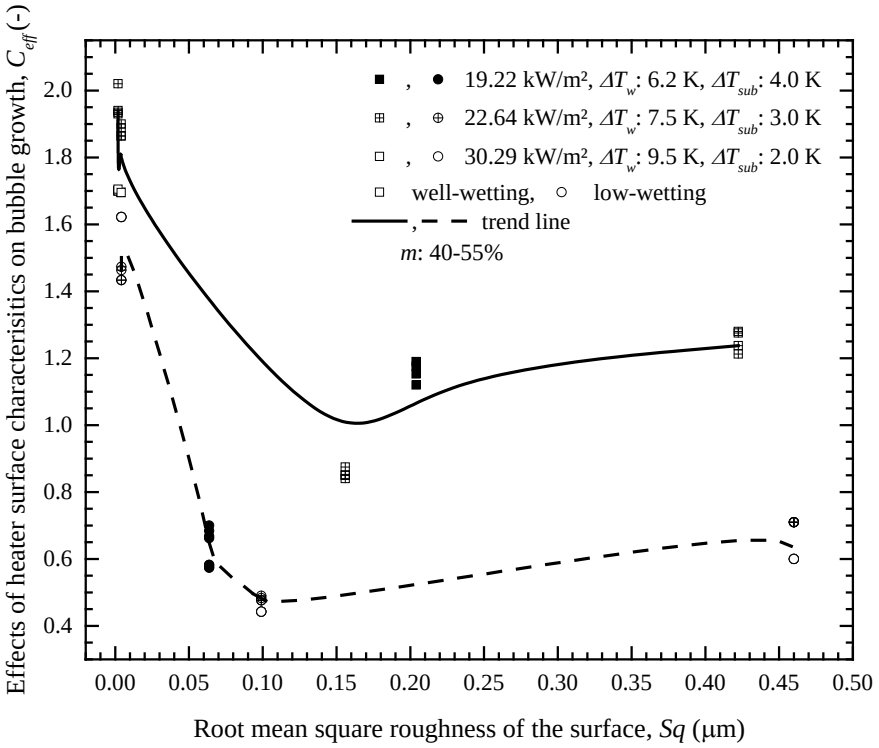

Fig. 8: Effects of heater surface characteristics on the effective microlayer constant (C_{eff}).

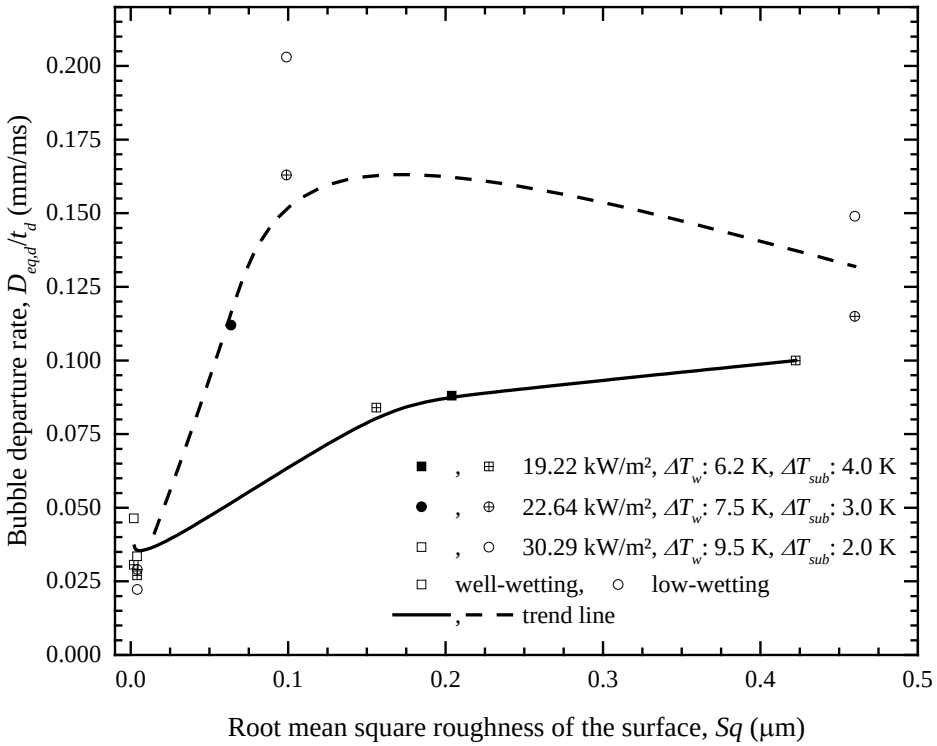

Fig. 9: Effects of heaters surface characteristics on the bubble growth rates before departure.

We may deduce the non-linear behavior of C_{eff} for different surface characteristics by analyzing Fig. 8 and Fig. 9 together. The solid and dashed lines of these figures are the best-fitting curves derived from the results generated by our proposed model (Fig. 8) and from the experimental results [23, 24] (Fig. 9). The B-spline curve fitting method is used in these cases. For smooth surfaces, the averaged bubble growth rate before departure is minimum (Fig. 9) and the effective microlayer thickness constant (C_{eff}) is maximum (Fig. 8). At the

optimal roughness of Sq=0.12 μm for low-wetting surfaces, the bubble growth rate is the greatest and C_{eff} is the lowest. The values of C_{eff} increase again and the bubble growth rates do not change much while the surface roughness is more than the optimal roughness (Sq=0.15μm) for well-wetting surfaces.

The expression for C_{eff} in our study is related to the thermo-hydrodynamic behavior of microlayer which exists beneath the nucleated bubble. According to our best knowledge, the existing theoretical analyses on the microlayer formation were performed for the plain surfaces [39, 43]. Several microscale CFD analyses and high resolution experiments attempted to reveal the underlying physics of the microlayer dynamics, where heater surfaces were also considered as smooth [16, 40, 41, 48]. The initial microlayer thickness was calculated by following different approaches; one of them was analyzing the approximate boundary layer [39, 42] and another one was solving the continuity and momentum equations of microlayer hydrodynamics [43]. A recent work by Jung and Kim [41] used the latter approach, as it includes a generalized form of the bubble growth behavior. The model is as follows

$$\frac{\partial u_m}{\partial t} + u_m \frac{\partial u_m}{\partial r} = -\frac{1}{\rho}\frac{\partial P}{\partial r} + \nu\left(\nabla^2 u_m - \frac{u_m}{r^2}\right). \quad (3)$$

Here u_m is the velocity at the microlayer boundary and $\frac{dP}{dR}$ was derived as a function of the bubble growth rate (dR/dt) using the Rayleigh-Plesset equation [49]. The theoretical models of initial microlayer thickness were the same form of $\delta_0 = C_2\left(\nu t_g\right)^{0.5}$. As mentioned earlier that different values of C_2 were derived by different groups. It means, C_2 includes the effects of different parameters, such as, fluid properties, system pressure, surface properties etc. In addition to the effects of bubble growth rate (dR/dt) on the microlayer, surface roughness and wettability may also influence the liquid flow in the microlayer due to the capillary pressure drop and the frictional pressure drop. Washburn [50] defined the capillary pressure by the term $\left(\frac{2\sigma\cos\theta}{0.5\,Xsm}\right)$, where θ is the liquid contact angle and X_{sm} is the distance between the consecutive surface profile peaks. Capillary wicking due to the surface profile gap was found to play significant role in rewetting of the dry spots [51]. According to the Washburn [50]'s equation, capillary pressure force would be greater for the low-wetting surfaces than that of the well-wetting surfaces. Therefore the microlayer thickness is supposed to be affected. Viscous pressure drop is also expected to be greater when the solid-liquid contact area is comparatively larger. Hence when the surface roughness height is greater than or equal to the microlayer thickness, results a greater frictional pressure drop.

Microlayer evaporation due to the nanoscale ridges (with the height of 0.3 μm to 1.5 μm) was experimentally investigated by Zou [52]. In this study, an idea of critical height of the ridges was hypothesized and validated against the experimental results. According to them, a thin liquid film beneath the bubble gets disconnected from the bulk liquid due to the ridge-structured surface. Evaporation of a film takes place when the input energy overcomes the energy barriers of liquid-liquid molecular attraction and solid-liquid attraction. Additional solid-liquid interfaces due to the extended surface profile replace the original liquid-liquid contact. As a result, the heat transfer is expedited, as the solid-liquid attraction is weaker than that of the liquid-liquid attraction. Along with the Zou [52], Sriraman [53] hypothesized the impacts of extended heater surface profiles on the microlayer evaporation. On these circumstances, the effects of heater surface characteristics (θ_{hys}, Sq) on the bubble growth, that is, the constant C_{eff} is explained based on the ideas of microlayer deformation [53], expressions of microlayer thickness [15, 54] and heat transfer through the microlayer [55].

Fig. 10 shows Sriraman [53]'s conceptual ideas of microlayer deformation. He postulated that on a smooth surface, the microlayer does not get disrupted during the bubble growth (Fig. 10b). Nano-fins unsettle the liquid microlayer when their heights are within the thickness of the liquid microlayer (Fig. 10c). If the length of nanofins exceeds the microlayer thickness, this leads to a disruption of the microlayer (Fig. 10d). The contact area between the liquid microlayer and the heater surface may increase due to the disturbed or disrupted microlayer. It can be added that the surface is partially submerged in the liquid microlayer for the maximum roughness height (Fig. 10d). Consequently, the portions of the roughness height outside the microlayer may hinder to expand the microlayer over the roughness. Thus the thickness of the microlayer may increases and raises the heat transfer resistance [23]. On the other hand, though the surface profile is perturbing the microlayer for the intermediate roughness (Fig. 10c), still liquid microlayer can expand over the roughness and effective heat transfer area increases. This gives a clear indication that the microlayer evaporation rate could be the maximum for the intermediate roughness. Sarker et al. [24] also found that the heat transfer to the bubble was the greatest due to the maximum microlayer evaporation rate at an intermediate roughness.

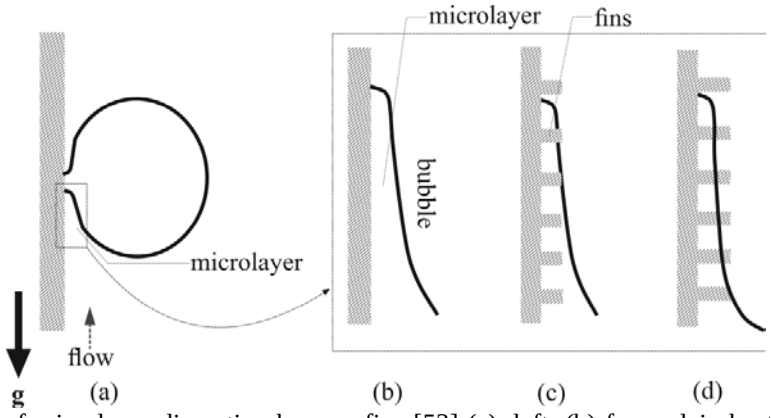

Fig. 10: Illustration of microlayer disruption by nanofins [53] (a), left: (b) for a plain heater surface, (c) for a surface profile submerged in the microlayer, (d) for a partially submerged surface profile.

Now we will deduce the relations of C_{eff} with the microlayer thickness and the heat conduction of the microlayer. If C_{eff} is used instead of C_2 in the expressions of initial microlayer thickness which are suggested by Cooper and Llyod [39] and Zhao et al. [54], they can be re-written as

$$\delta_{ml,0}=C_{eff}\left(\nu t_g\right)^{0.5}=\frac{C_{eff}^2 Pr\alpha\rho_v h_{fg} r}{2k_l\Delta T_{sat}}. \tag{4}$$

Chen et al.[55] calculated the heat flux of microlayer evaporation by

$$q''_{ml}=\frac{\left(T_w-T_i\right)}{\delta_{ml}/k_l+1/h_i} \tag{5}$$

Here t_g is the bubble growth time to the point considered, T_i is the temperature of the vapour-liquid interface and h_i is the interfacial evaporation heat transfer coefficient. Eq. 4 shows that the initial microlayer thickness reduces when C_{eff} is lower and that results the greater microlayer evaporation (Eq. 5). The hypothesis of microlayer deformation [53] suggested that the microlayer evaporation rate is greater at the intermediate/optimal roughness. This concludes that the effect of heater surface characteristics on the bubble growth (C_{eff}) is the lowest for the intermediate roughness height which we can see in Fig. 8. Moreover, since the surface tension forces at the three-phase contact line work outward for the low-wetting surfaces, the bubble base area during the initial bubble growth period is greater on such surfaces [23]. Therefore, the heat transfer rate through the microlayer is the greatest at the roughness of Sq =0.12 μm for low-wetting surfaces. Based on the two distinguishable curves of Fig. 8, we performed an exponential regression analysis and found the expressions for C_{eff} as follows

For well-wetting surfaces:

$$P_1\left(\exp\left(-\frac{Sq/Sq_{crit}}{P_2}\right)+P_3\left(\frac{Sq}{Sq_{crit}}\right)+P_4\right)\left(\frac{\theta_{crit}}{\theta_{hys}}\right)^{P_5}. \tag{6(a)}$$

For low-wetting surfaces:

$$P_1\left(\exp\left(-\frac{Sq/Sq_{crit}}{P_2}\right)+P_3\left(\frac{Sq}{Sq_{crit}}\right)+P_4\right)\left(\frac{\theta_{hys}}{\theta_{crit}}\right)^{P_5}. \tag{6(b)}$$

Sq_{crit}=0.13 μm, θ_{crit}=90°.

In the above two equations, P_1=1.90, P_2=0.55, P_3=0.24, P_4=0.30 and P_5=0.13. It is to be noted that the expressions (Eqns. 6 a, b) are limited to the experimental boundary conditions of our experiments [23, 24].

5. Conclusion

Heater surface characteristics play an important role in the bubble departure process during the nucleate boiling. Existing bubble growth models do not extensively include the heater surface characteristics. In this study, we have formulated a bubble growth model incorporating most plausible mechanisms stated by different groups. Bubble sizes were calculated using this formulation and validated against the experimental results. The proposed bubble growth model consists of three constants for the contributions of three different heat transfers in the bubble growth, such as, the effective microlayer thickness constant (C_{eff}) for microlayer evaporation, $\acute{b}$ for the liquid inertia and heat diffusion through the bubble surface and the portion of a bubble in contact with the subcooled liquid ($\acute{S}$) for condensation heat transfer at the bubble cap. We have calculated C_{eff} for different portions of bubble in contact with the subcooled liquid ($\acute{S}$=0.35~0.65 or m=40%~55%) by keeping $\acute{b}$ constant ($\acute{b} = \pi/7$) [31] .

The effective microlayer thickness constant (C_{eff}) defines the influence of heater surface characteristics on the bubble growth rates during nucleate boiling. C_{eff} is found lower for the roughness of Sq=0.12 μm and Sq=0.15 μm for the low- and well-wetting surfaces, respectively. Finally, an expression of C_{eff} is proposed as a function of root mean square roughness of the surface (Sq) and the surface wettability (θ_{hys}). This expression can be used in the bubble growth models to predict the effects of heater surface characteristics on the bubble departure as well.

Conflict of Interest

There is no conflict of interest.

References

[1] J. W. S. Rayleigh, On the pressure developed in a liquid during the collapse of a spherical cavity. Philosophical Magazine Series 6, 1917. **34**: p. 94-98.

[2] Y. Lien, P. Griffith, The bubble growth at reduced pressure. 1969, Massachusetts Institute of Technology.

[3] A. J. Robinson, R. L. Judd, Bubble growth in a uniform and spatially distributed temperature field. International Journal of Heat and Mass Transfer, 2001. **44**: p. 2699-2710.

[4] F. Mayinger. Advanced experimental methods. in International Conference on Convective Flow Boiling. 1995. Alberta, Canada: Taylor & Francis.

[5] J. Liao, R. Mei, J. Klausner, The Influence of the bulk liquid thermal boundary layer on saturated nucleate boiling. International Journal of Heat and Mass Transfer, 2004. **25**: p. 196-208.

[6] N. Zuber, The dynamics of vapor bubbles in nonuniform temperature fields. International Journal of Heat and Mass Transfer, 1961. **2**: p. 83-98.

[7] M. S. Plesset, S. A. Zwick, The growth of vapor bubbles in superheated liquids. Journal of Applied Physics, 1954. **25**(4): p. 493-500.

[8] H. K. Forster, N. Zuber, Dynamics of vapor bubbles and boiling heat transfer. American Institute of Chemical Engineers, 1955. **1**(4): p. 531-535.

[9] Scriven, L.E., On the dynamics of phase change. Chemical Engineering Science, 1959. **10**: p. 1-13.

[10] L. D. Koffman, M. S. Plesset, Experimental observations of the microlayer in vapor bubble growth on a heated solid. Journal of Heat Transfer, 1983. **108**: p. 625-632.

[11] S.B. Jung, H.D. Kim, An experimental method to simultaneously measure the dynamics and heat transfer associated with a single bubble during nucleate boiling on a horizontal surface. International Journal of Heat and Mass Transfer, 2014. **73**: p. 365-375.

[12] T. Yabuki, O. Nakabeppu, Heat transfer mechanisms in isolated bubble boiling of water observed with MEMS sensor. International Journal of Heat and Mass Transfer, 2014. **76**: p. 286-297.
[13] A. Mukherjee, S.G. Kandlikar, Numerical study of single bubbles with dynamic contact angle during nucleate pool boiling. International Journal of Heat and Mass Transfer, 2007. **50**: p. 127-138.
[14] T. Yabuki, T. Hamaguchi, O. Nakabeppu, Interferometric measurement of the liquid-phase temperature field around an isolated boiling bubble. Journal of Thermal Science and Technology, 2012. **7**: p. 463-474.
[15] M.G. Cooper, The microlayer and bubble growth in nucleate pool boiling. International Journal of Heat and Mass Transfer, 1969. **12**: p. 915-933.
[16] Y. Sato, B. Niceno, A depletable micro-layer model for nucleate pool boiling. Journal of Computational Physics, 2015. **300**: p. 20-52.
[17] A. Zou, D. P. Singh, S. C. Maroo, Early evaporation of microlayer for boiling heat transfer enhancement. Langmuir, 2016. **32**: p. 10808-10814.
[18] S. H. Kim, G.C.L., J. Y. Kang, K. Moriyama, H. S. Park, M. H. Kim, A study of nucleate bubble growth on microstructured surface through high speed and infrared visualization. International Journal of Multiphase Flow, 2017. **95**: p. 12-21.
[19] S. Maity, Effect of velocity and gravity on bubble dynamics, U.o. California, Editor. 2000.
[20] B.J. Jones, J.P. McHale, S.V. Garmella, The infuenece of surafce roughness on nucleate pool boiling heat transfer. Journal of Heat Transfer, 2009. **131**.
[21] H.T. Phan, N. Caney, P. Marty, S. Colasson, J. Gavillet, Surface wettability control by nanocoating: The effects on pool boiling heat transfer and nucleation mechanism. International Journal of Heat and Mass Transfer, 2009. **52**: p. 5459-5471.
[22] Y. Nam, J. Wu, G. Warrier, Y.S. Ju Experimental and numerical study of single bubble dynamics on a hydrophobic surface. Journal of Heat Transfer, 2009. **131**(12).
[23] D. Sarker, R. Franz, W. Ding, U. Hampel, Single bubble dynamics during subcooled nucleate boiling on a vertical heater surface: An experimental analysis of the effects of surface characteristics. International Journal of Heat and Mass Transfer, 2017. **109**: p. 907-921.
[24] D.Sarker, W.Ding, R.Franz, O.Varlamova, P.Kovats, K.Zähringer, U.Hampel, Investigations on the effects of heater surface characteristics on the bubble waiting period during nucleate boiling at low subcooling. Experimental Thermal and Fluid Science, 2019. **101**: p. 76-86.
[25] R. Mei, W. Chen, J. F. Klausner, Vapor bubble growth in heterogeneous boiling -I. formulation. International Journal of Heat and Mass Transfer, 1995. **38(**5): p. 909-919.
[26] S. J. D. van Stralen, M. S. Sohal, R. Cole, W. M. Sluyter, Bubble growth rates in pure and binary systems: combined effect of relaxation and evaporation microlayers. International Journal of Heat and Mass Transfer, 1975. **18**: p. 453-467.
[27] Y. M. Chen, F. Mayinger, Measurement of heat transfer at the phase interface of condensing bubbles. International Journal of Multiphase Flow, 1992. **28**(6): p. 877-890.
[28] S. Narayan, A. Srivastava, S. Singh, Rainbow schlieren-based investigation of heat transfer mechanisms during isolated nucleate pool boiling phenomenon : Effect of superheat levels. International Journal of Heat and Mass Transfer, 2018. **120**: p. 127-143.
[29] B. J. Yun, A. Splawski, S. Lo, C.H. Song, Prediction of a subcooled boiling flow with advanced two-phase flow models. Nuclear Engineering Design, 2012. **253**: p. 351-359.
[30] M. Colombo, M. Fairweather, Prediction of bubble departure in forcd convection boiling: A mechanistic model. International Journal of Heat and Mass Transfer, 2015. **85**: p. 135-146.
[31] B. B. Mikic, W. M. Rohsenow, P. Griffith, On bubble growth rates. International Journal of Heat and Mass Transfer, 1970. **13**: p. 657-666.
[32] S. Raj, M. Pathak, M. K. Khan, An analytical model for predicting growth rate and departure diameter of a bubble in subcooled flow boiling. International Journal of Heat and Mass Transfer, 2017. **109**: p. 470-481.
[33] T. Mazzocco, W. Ambrosini, R. Kommojosyula, E. Baglietto, A reassessed model for mechanistic prediction of bubble departure and lift off diameters. International Journal of Heat and Mass Transfer, 2018. **117**: p. 119-124.
[34] Y. Nam, E. Aktinol, V.K. Dhir, Y. S. Ju, Single bubble dynamics on a superhydrophilic surface with artificial nucleation sites. International Journal of Heat and Mass Transfer, 2011. **54**: p. 1572-1577.
[35] C.C. Hsu, T.W. Su, P.H. Chen, Pool boiling of nanoparticle-modified surface with interlaced wettability. Nanoscale Research Letters, 2012. **7**.
[36] H.J. Jo, S.H. Kim, H. Kim, M. H. Kim, Nucleate boiling performance on nano/microstructures with different wetting surfaces. Nanoscale Research Letters, 2012. **7**.

[37] M. G. Cooper, A. J. P. Lloyd, The microlayer in nucleate pool boiling. International Journal of Heat and Mass Transfer, 1969. **12**: p. 895-913.
[38] M. Gao, L. Zhang, P. Cheng, X. Quan, An investigation of microlayer beneath nucleation bubble by laser intereometric method. International Journal of Heat and Mass Transfer, 2012. **57**: p. 183-189.
[39] M.G. Cooper, A.J.P. Lloyd, The microlayer in nucleate pool boiling. International Journal of Heat and Mass Transfer, 1969. **12**: p. 895-913.
[40] S. Hänsch, S. Walker, The hydrodynamics of microlayer formation beneath vapour bubbles. International Journal of Heat and Mass Transfer, 2016. **102**: p. 1282-1292.
[41] S. Jung, H. Kim, Hydrdynamic formation of a microlayer underneath a boiling bubble. International Journal of Heat and Mass Transfer, 2018. **120**: p. 1229-1240.
[42] H.J. van Ouwerkerk, The rapid growth of a vapour bubble at a liquid-solid interface. International Journal of Heat and Mass Transfer, 1971. **14**: p. 1415-1431.
[43] G. F. Smirnov, Calculation of the "initial" thickness of the "microlayer" during bubble boiling. Journal of Engineering Physics, 1975. **28**: p. 369-374.
[44] W. E. Ranz, W. R. Marshall, Evaporation from drops - Part II. Chemical Engineering Progress, 1952. **48**(4): p. 173-180.
[45] Y. H. Zhao, T. Tsuruta, T. Masuoka, Critical heat flux prediction of subcooled pool boiling based on the microlayer model. JSME International Journal, 2002. **45**(3): p. 712-718.
[46] U. Harm, W. Fürbeth, K.-M. Mangold, K. Jüttner, Novel protective coatings for steel based on a combination of self-assembled monolayers and conducting polymers, in Macromolecular Symposia. 2002. p. 65-76.
[47] O. Varlamova, K. Hoefner, M. Ratzke, J. Reif, D. Sarker, Modification of surface properties of solids by femtosecond LIPSS writing: comparative studies on silicon and stainless steel. Applied Physics A, 2017. **123**(725).
[48] G. Giustini, S. Jung, H. Kim, S.P. Walker, Evaporative thermal resistance and its influence on microscopic bubble growth. International Journal of Heat and Mass Transfer, 2016. **101**: p. 733-741.
[49] M. S. Plesset, The dynamics of cavitation bubbles. Journal of Applied Mechanics, 1949. **16**: p. 277-282.
[50] E.W. Washburn, The Dynamics of Capillary Flow. Physical Review, 1921. **17**.
[51] S. H. Kim, H. C. Lee, J. Y. Kang, K. Moriyama, M. H. Kim, H. S. Park, Boiling heat transfer and critical heat flux evaluation of the pool boiling on microstructured surface. International Journal of Heat and Mass Transfer, 2015. **91**: p. 1140-1147.
[52] A. Zou, Fundamentals of microlayer evaporation and its role on boiling heat transfer enhancement, in SURFACE, S. University, Editor. 2015.
[53] S.R. Sriraman, Pool Boiing on Nano-Finned Surfaces, T.A.M. University, Editor. 2007.
[54] Y.-H. Zhao, T.M., T. Tsuruta, Unified theoretical prediction of fully developed nucleate boiling and critical heat flux based on a dynamic microlayer model. International Journal of Heat and Mass Transfer, 2002. **45**: p. 3189-3197.
[55] Z. Chen, F. Wu, Y. Utaka, Numerical simulation of thermal property effect on heat transfer plate on bubble growth with microlayer evaporation during nucleate pool boiling. International Journal of Heat and Mass Transfer, 2018. **118**: p. 989-996.